

28.2 A 220 μ W -85dBm Sensitivity BLE-Compliant Wake-up Receiver Achieving -60dB SIR via Single-Die Multi-Channel FBAR-Based Filtering and a 4-Dimensional Wake-Up Signature

Po-Han Peter Wang, Patrick P. Mercier

University of California, San Diego, La Jolla, CA

Wake-up receivers (WuRXs) offer an attractive low-power means to synchronize low-average-throughput wireless devices without requiring energy-expensive periodic synchronization routines between primary radios. To achieve low-power operation, most prior-art WuRXs tend to utilize custom OOK or FSK modulation schemes that are not compliant with any standards, while also forgoing important capabilities present in more powerful radios, such as the ability to operate in the presence of potentially large interferers or dynamically switch between multiple channels – both of which are very important when operating in congested bands. Since Bluetooth Low Energy (BLE) is one of the most popular standards for low-power IoT devices, prior work has endeavored to develop BLE-compliant WuRXs that achieve low-power operation through means of back-channel (BC) communication – signals that are generated by a standard-compliant BLE TX, yet encode information in a modality that can be demodulated by low-power means (e.g., direct energy detection [1,2]). Unfortunately, the wideband energy detectors in [1,2] not only directly demodulate interferers with no channel selectivity, they also introduce significant demodulated RF noise, limiting sensitivity to -56.5dBm at 236nW and -58dBm at 164 μ W, respectively. To impart channel selectivity, a mixer-first architecture was demonstrated in [3], achieving a sensitivity of -80dBm at 230 μ W, though this does not include the power of a PLL or FLL to stabilize the free-running single-channel VCO. To facilitate stabilized multichannel operation, a 120 μ W crystal-stabilized FLL-based LO generator was included in [4] with frequency hopping support, for a total WuRX power of 150 μ W. While selective, the design achieved a sensitivity of only -57.5dBm.

This paper presents a BLE-compliant WuRX, shown in Fig. 28.2.1, that achieves -85dBm sensitivity at 220 μ W while supporting multichannel frequency diversity and interference resiliency by: 1) employing a single-die 0.25mm² 3-channel FBAR for direct filtering of the 3 BLE advertisement channels; 2) integrating the energy in each advertisement channel via a frequency-hopping time-counting majority-voting algorithm for low-cost BLE-compliant energy-detection-based demodulation over four distinct dimensions; 3) mixing each advertisement channel down to low-IF prior to energy-detection via a two-stage heterodyne structure for further channel filtering and adjacent channel rejection; and 4) implementing the 3-channel LO generator via an ultra-low-power crystal-stabilized integer- N PLL with frequency tripler.

The block diagram of the WuRX is shown in Fig. 28.2.1. After 9dB of passive voltage gain, RF signals are filtered by the 3-channel single-die FBAR filter, a single channel of which is selected via an integrated SP3T switch that, via an on-resistance of 16.7 Ω , degrades the Q of the FBAR from 1040 to 370. As shown in Fig. 28.2.2, an RF LO, centered 8MHz lower than the channel, is used to downconvert one of the 3 channels to an 8MHz IF. The LO for the three BLE advertisement channels at 2402, 2426, and 2480MHz are generated in a low-power manner via an integer- N PLL, shown in Fig. 28.2.2 (bottom), that takes an 8MHz crystal reference, divides it by 4, and compares to an oscillator that, instead of operating at 2.4GHz, operates at 798, 806, or 824MHz via divider ratios of N ={399, 403, 412} to save power; the final LO frequency is subsequently generated via an AND-based frequency-tripling edge combiner, enabled via the naturally-occurring multiple phases in the ring oscillator. As part of the tripler, the LO drives a 2-phase 6-switch passive mixer, the output of which passes through an inverter-based IF amplifier. The IF signal is then, thanks to the careful frequency planning, easily mixed to baseband via the 8MHz crystal reference and an N -path filtering passive mixer. Fortunately, the 500kHz-spaced FSK tones generated by the BLE standard are, for the purposes of energy detection, self-images of each other when centered around the 8MHz IF LO, and thus a 3-stage lowpass filter and a 27-to-45dB gain PGA are used to condition the 250kHz downconverted signal. Envelope detection is then performed by a cross-coupled self-mixing envelope detector (ED) to provide a pseudo-differential BB signal and forgo the need of a precise voltage reference for the following 25 \times oversampled 2-stage dynamic comparator, which utilizes capacitive trimming to set the comparison threshold.

An on-chip digital baseband and finite state machine (FSM) are used to parse BB data to decide if a wake-up signature is detected. Similar to [2], two dimensions

are used to detect the presence of an advertisement packet at a single frequency: the packet must meet a minimum power threshold defined by both the PGA and the comparator threshold, and be within a pre-specified packet length tolerance between T_L and T_H , which are the lower and upper bound of the targeted packet length (a single BLE packet length can be between approximately 128 and 376 μ s with 1 μ s steps). Unlike [2], however, and in a similar manner to [4], though here with majority-voting and with an on-chip digital BB, two additional dimensions are added to the WuRX: channel frequency, and the hopping time between channels. The on-chip FSM begins by detecting energy in Channel 37. If the correct single-channel signature is received, the FSM moves to Channel 38, and then Channel 39 according to desired timing, which is programmable. If Channel 38 has an overlapping Wi-Fi or BLE blocker whose packet is longer than desired, as illustrated in Ex. 1 in Fig. 28.2.1, Channel 38 will miss detection, but if Channels 37 and 39 hit, the 4-dimensional wake-up signature is still detected. The 4D signature also helps prevent false alarms – for example, if Channel 37 hits due to a blocker, yet Channels 38 and 39 do not, no false alarm is observed as illustrated in Ex. 2 in Fig. 28.2.1. There are over 38,000 possible signatures available to decode in this design. The state machine diagram governing the sequencing behavior is shown in Fig. 28.2.3.

The BLE-compatible WuRX was fabricated in 65nm CMOS, and a single-die 3-channel FBAR is stacked and wirebonded on top. The FBAR filters have 3dB bandwidths of 9.7MHz, temperature coefficients of 0.89 ppm/ $^{\circ}$ C [5], and bondwire length variation can alter the center frequency by up to 200kHz/100 μ m. Figure 28.2.4 (top left) shows the measured S_{11} of the WuRX when configured to operate in each of the advertisement channels, demonstrating the frequency-selectivity of the FBARs. The output of the PLL before the edge combiner is shown in Fig. 28.2.4 (top right). With the entire system operating together, the WuRX achieves a sensitivity of -85dBm for a missed detection rate of 10^{-3} and a false-alarm rate less than once per half hour, as shown in Fig. 28.2.4 (bottom left). The filtering characteristics of the FBAR and the heterodyne structure help a single channel achieve a signal-to-interference ratio of -23dB at a 10MHz offset (Fig. 28.2.4, bottom right). If the FBAR notch were placed at 16 instead of 27MHz offset, it would have improved image rejection by a further ~10dB; this can be easily rectified by FBAR tuning. More importantly, however, the frequency-hopping voting scheme enables extremely large blockers to be located near any single channel. Testing to the limit of the employed signal generator revealed that, with frequency-hopping voting, up to -60dB SIR could be achieved for both BLE and 802.11g Wi-Fi jammers, with that number likely to be higher with availability of more capable test equipment.

To validate realistic use, the WuRX was connected to an antenna in a normal lab environment and was demonstrated to wake up from a commercial mobile phone, yet the WuRX did not wake up when an adjacent phone transmitted packets of a different length, as shown in Fig. 28.2.5 (top). The WuRX also woke up correctly when two phones playing videos over Wi-Fi were placed next to the antenna, while a phone that delivered the BLE advertisement packets was placed upwards of 10m away (1m shown in Fig. 28.2.5, bottom for clarity). During continuous operation, the WuRX consumes 220 μ W. According to Fig. 28.2.6, the proposed WuRX achieves the best sensitivity and highest amount of interference rejection amongst all BLE-compatible WuRXs at comparable power consumption in the table. A photograph of the die-stacked WuRX is shown in Fig. 28.2.7.

Acknowledgements:

The authors would like to acknowledge Broadcom Inc. for providing the FBAR die.

References:

- [1] N. E. Roberts et al., "A 236nW -56.5dBm-Sensitivity Bluetooth Low-Energy Wakeup Receiver with Energy Harvesting in 65nm CMOS," *ISSCC*, pp. 450-451, Feb. 2016.
- [2] M. Ding et al., "A 2.4GHz BLE-Compliant Fully-Integrated Wakeup Receiver for Latency-Critical IoT Applications Using a 2-Dimensional Wakeup Pattern in 90nm CMOS," *IEEE RFIC*, pp. 168-171, June 2017.
- [3] M. R. Abdelhamid et al., "A -80dBm BLE-Compliant, FSK Wake-up Receiver with System and Within-Bit Duty Cycling for Scalable Power and Latency," *IEEE CICC*, pp. 1-4, April 2018.
- [4] A. Alghaihab et al., "A 150 μ W -57.5 dBm-Sensitivity Bluetooth Low-Energy Back-Channel Receiver with LO Frequency Hopping," *IEEE RFIC*, pp. 324-327, June 2018.
- [5] K. Wang et al., "Design of 1.8-mW PLL-Free 2.4-GHz Receiver Utilizing Temperature-Compensated FBAR Resonator," *IEEE JSSC*, vol. 53, no. 6, pp. 1628-1639, June 2018.

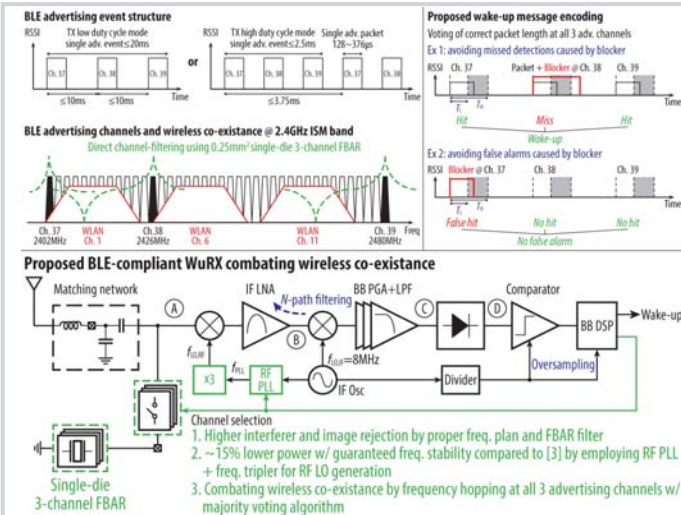


Figure 28.2.1: BLE advertising event structure, channel allocation, and frequency hopping wake-up messages (top); proposed interference-resilient BLE-compliant WuRX architecture (bottom).

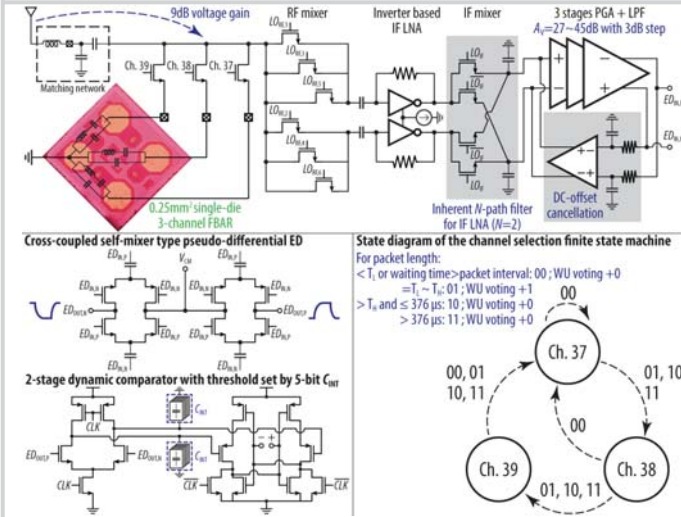


Figure 28.2.3: Schematic of proposed WuRX signal chain (top and bottom left); state diagram of the proposed majority-voting channel selection algorithm for 4D wake-up signature detection (bottom right).

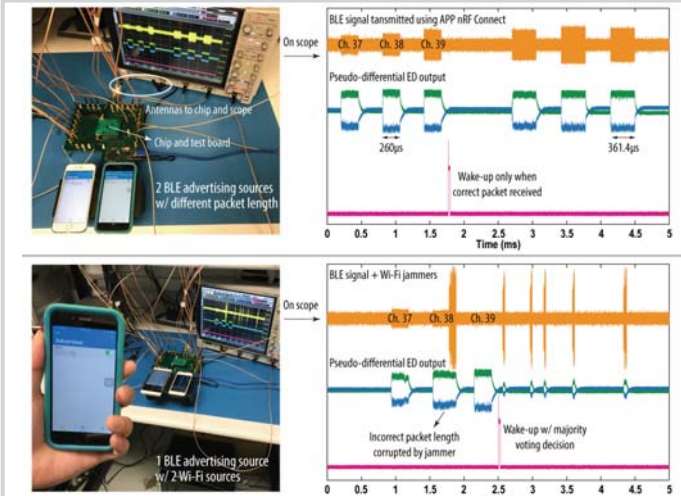


Figure 28.2.5: Demonstration of correct wake-up using mobile phones by sending: 1) two different BLE advertising packets with different packet lengths (top), and 2) BLE packets alongside two proximal Wi-Fi jammers (bottom).

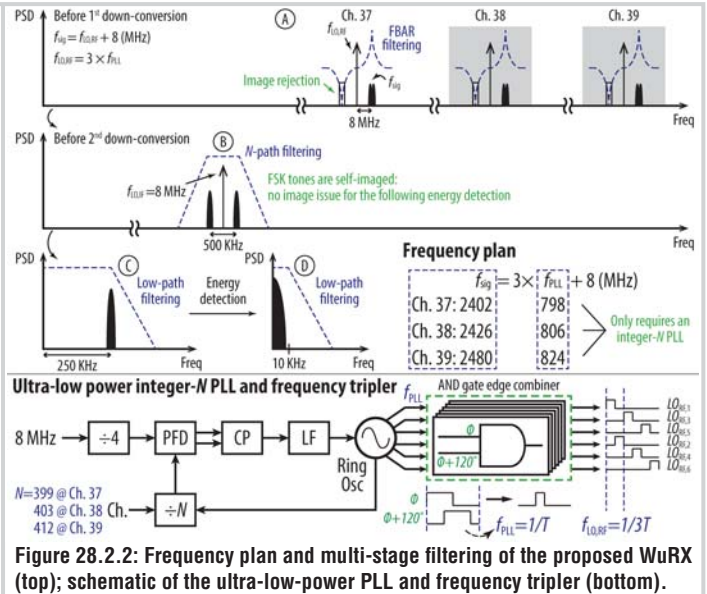


Figure 28.2.2: Frequency plan and multi-stage filtering of the proposed WuRX (top); schematic of the ultra-low-power PLL and frequency tripler (bottom).

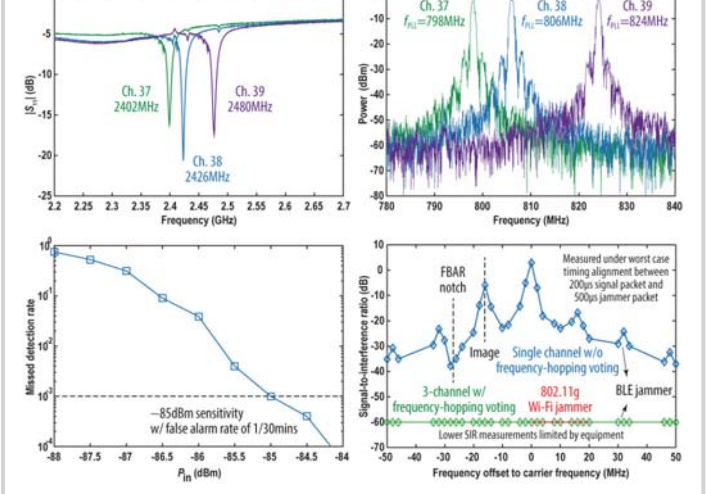


Figure 28.2.4: Measurement results of |S₁₁|, PLL locking frequency, missed detection rate waterfall curve, and signal-to-interference ratio using modulated BLE and 802.11g Wi-Fi jammers.

Power breakdown

IF LNA	IF PGA	Comparator	PLL + frequency tripler (including LO buffers)	Digital baseband
22.4µW	22.2µW	2.7µW	166.2µW	6.1µW

	Roberts ISSCC'16	Ding RFIC'17	Abdelhamid CICC'18	Alghahab RFIC'18	This Work
Technology	65nm	90nm	65nm	65nm	65nm
Die area	2.25mm ²	1.24mm ²	4mm ²	1.1mm ²	2.4mm ²
Supply voltage	1.0.5V	2V	0.75V	1.1 / 0.9V	0.5V
WuRX decoding	Interval and duration of adv. events	Packet duration + RSSI	GFSK	3 channels detection + BC symbol correlation	3 channels voting + packet length + packet interval + power threshold
BLE compatible frequency hopping	No	No	No	Yes	Yes
Frequency locked demodulation	N/A ¹	N/A ¹	No	Yes	Yes
Integrated digital baseband	Yes	Yes	Yes	No	Yes
Adjacent channel SIR @ 2MHz	N.R. ²	N.R. ²	N.R. ²	-4dB	-6dB ¹ / -60dB ⁴
Adjacent channel SIR @ 10MHz	N.R. ²	N.R. ²	N.R. ²	-20dB	-23dB ¹ / -60dB ⁴
RX power	236µW	164µW	230µW	150µW	220µW
Latency	-2s	-100µs	-200µs	1.47ms ⁵	-200µs ¹ / 1.47ms ^{4,5}
Sensitivity	-56.5dBm	-58dBm	-80dBm	-57.5dBm	-85dBm
FoM ⁶	89.3dB	105.9dB	123.4dB	94.1dB	128.6dB ¹ / 119.9dB ⁴

¹ Not applicable.
² Not reported.
³ Single channel w/o frequency hopping mode enabled.
⁴ 3 channels w/ frequency hopping mode enabled.
⁵ 1 advertising event, use UUID=0x180D here for example.
⁶ FoM (dB) = -P_{rx} + 10log(1/Latency) - 10log(P_{rx}/mW)

Figure 28.2.6: Power breakdown of the proposed WuRX (top), and comparison to state of the art (bottom).

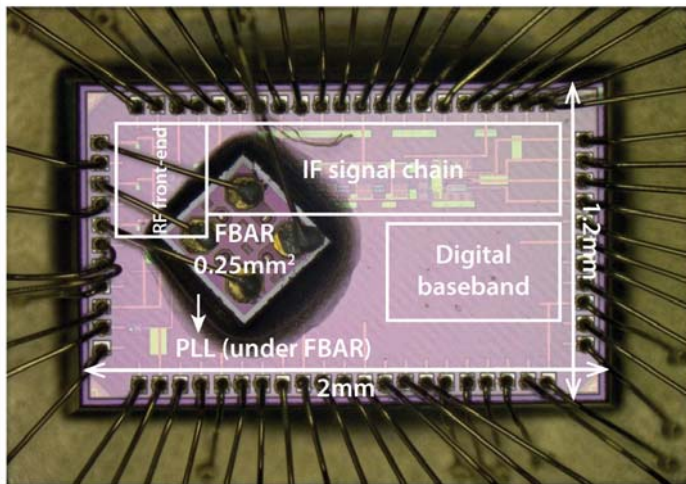


Figure 28.2.7: Die micrograph of the WuRX employing a single-die 3-channel FBAR stacked on top of the WuRX die.